Removal of hexavalent chromium by anion exchange: Non-target anion behavior and practical implications

Leah C. Flint[1,2], Miguel S. Arias-Paić[2], Julie A. Korak[1*]
[1]Department of Civil, Environmental, and Architectural Engineering, University of Colorado Boulder, UCB 607, Boulder, CO 80303
[2]Bureau of Reclamation, Department of the Interior, PO Box 25007, Denver, CO 80225

Supporting Information

1 Methods

1.1 Safety

There were several chemical safety hazards during regeneration and batch experiments. PPE, careful sample handling, and workplace hygiene were necessary to mitigate risks. Ion exchange concentrates metals that are present at trace concentrations in the raw water by accumulating mass during loading and releasing metals at high concentrations during regeneration. Regeneration waste brine contains hazardous concentrations of hexavalent chromium, arsenic, vanadium, uranium, and selenium. Regeneration samples were handled and disposed as hazardous waste. Inefficient regeneration also leaves uranium on the resin requiring hazardous waste disposal. Batch regeneration also used concentrated solutions of hydrochloric acid, which is corrosive and a chemical hazard.

1.2 Experimental Design

Three strong base resins were tested in this study. The specifications for each resin, as reported by the manufacturers, are summarized in Table S 1. A process and instrumentation diagram (P&ID) for the five-column system used to load the A600E columns is shown in Figure S 1. The PGW6002E and TP107 columns were loaded in a similar system with two pairs of columns arranged in a lead-lag configuration. Only the lead columns were analyzed.

Table S 1. Resin properties reported by the manufacturer for each resin

Resin	Purolite A600e/9149 (A600E)	Purolite PGW6002E (PGW6002E)	Lanxess Lewatit TP 107 (TP107)
Delivery Form	Cl^-		
Functional Group	Quaternary Ammonium		
Polymer Structure	Type I gel polystyrene with divinylbenzene crosslinking		Macroporous polyacrylic with crosslinking
Effective Size [mm]	0.52-0.62		0.49-0.65
Water Retention (Cl^-form) [% wt.]	43-48%	40-45%	30-42%
Total Capacity [eq/L]	1.6	1.65	2.4

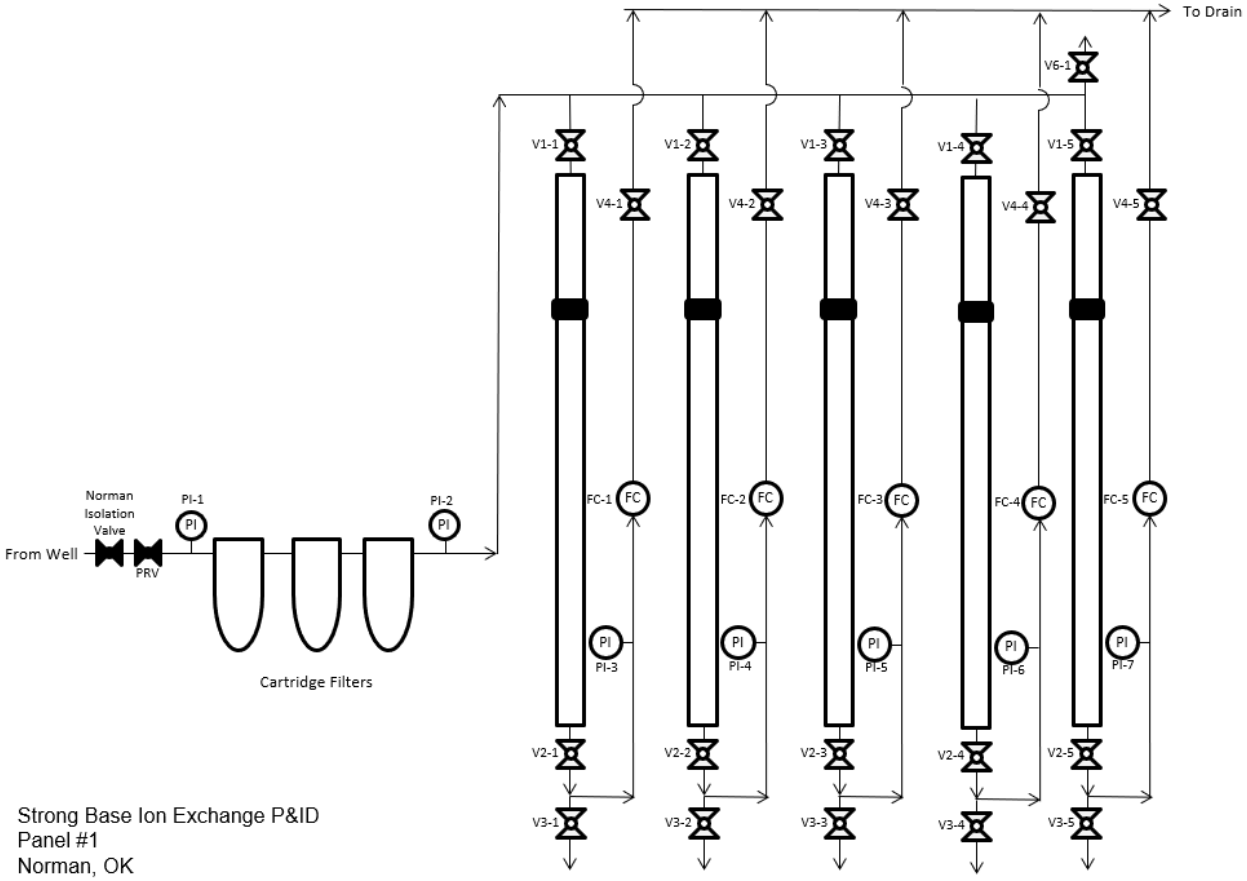

Figure S 1. Process and instrumentation diagram (P&ID) for single pass loading with five columns in parallel

1.3 **Influent Water Quality**

Raw groundwater collected after cartridge filtration was evaluated during both initial loading and reloading for bulk water quality, major cations, major anions, and trace metals (Table S 2). High frequency samples were collected during A600E C6 loading and evaluated for trace metals.

Table S 2: Influent water quality at well site. Laboratory and method information from Table S 5 and Table S 6. Concentration reported as average ± 95% confidence interval.

Parameter	Concentration	Sampling Events
pH (s.u.)	8.3 ± 0.1	3
Total Alkalinity (mg/L as $CaCO_3$)	265 ± 24	4
DO (mg/L)	6.5 ± 0.8	3
TDS (mg/L)	362 ± 36	3
Conductivity (µS/cm)	536 ± 7	3
Dissolved Organic Carbon (mg/L)	1.0 ± 0.1	4
Calcium (mg/L)	8.39 ±0.38	4
Potassium (mg/L)	1.94 ± 0.10	4
Magnesium (mg/L)	4.95 ± 0.22	4
Sodium (mg/L)	104 ± 6	4
Chloride (mg/L)	17.0 ± 0.4	4
Sulfate (mg/L)	13.6 ± 1.2	4
Nitrate-Nitrite (mg/L as N)	0.30 ± 0.03	7
Iron, Total (mg/L)	<0.025	4
Manganese, Total (mg/L)	<0.001	4
Arsenic, Total (µg/L)	6.6 ±0.2	16
Molybdenum, Total (µg/L)	3.4 ± 0.3	11
Selenium, Total (µg/L)	19.4 ± 0.7	11
Vanadium, Total (µg/L)	99.5 ± 2.1	16
Uranium, Total (µg/L)	13.4 ± 0.2	14

Cr(T) and Cr(VI) concentrations in raw groundwater were evaluated 9 and 11 times, respectively, during fresh resin loading and regenerated resin reloading. Cr(VI) ranged from 92 to 103% of total chromium for four samples analyzed for both parameters, with three samples having higher Cr(VI) concentrations than Cr(T). Cr(T) concentrations were assumed to be adequate for Cr(VI) concentrations, and only Cr(T) was evaluated for A600E C6 loading and reloading. The average influent concentrations and corresponding 95% confidence intervals based on all measurements collected during column loading periods was 86.1 ± 3.8 µg/L (Table S 3). Average influent concentrations during A600E C1-C5 (n=10) and C6 (n=5) loading periods were 87.0 ± 1.2 and 89.6 ± 2.9 µg/L, respectively. Chromium concentration was measured once during PGW6002E and TP107 loading as 88.3 µg/L. Split samples for influent Cr(T) were analyzed at CU Boulder and Analab and found to agree within 5%.

Table S 3. Influent chromium at well site

Loading Period	Metric	Units	Total Chromium	Hexavalent Chromium	Overall*
A600E C1-C5	Average	µg/L	85.8	87.6	87
	RSD	%	0.4%	1.2%	1.4%
	Count	–	3	10	10
	95% Confidence Interval	µg/L	85.4 – 86.2	87.0 – 88.2	86.3 – 97.7
PGW6002E/TP107	Average	µg/L	88.3	81.5	88.3
	RSD	%	-	-	-
	Count	–	1	1	1
A600E C6	Average	µg/L	89.6	-	89.6
	RSD	%	3.2%	-	3.2%
	Count	–	5	-	5
	95% Confidence Interval	µg/L	87.1 – 92.1	-	87.1 – 92.1
Reloading (All Resins)	Average	µg/L	82	-	82
	RSD	%	4.2%	-	4.2%
	Count	–	7	-	7
	95% Confidence Interval	µg/L	79.5 – 84.5	-	79.5 – 84.5
All Measurements	Average	µg/L	85.5	87.0	86.1
	RSD	%	5.1%	2.4%	4.4%
	Count	–	16	11	23
	95% Confidence Interval	µg/L	83.3 – 87.6	85.8	84.6 – 87.6
*Overall calculation includes all samples measured for Cr(T) and samples measured for Cr(VI) that were not collected at the same time as a Cr(T) sample.					

1.4 **Batch Tests Using Pilot Column Samples**

In addition to the batch test procedure described in the main text (Section 2.4), eight 10 mL aliquots of resin were extracted from the top and bottom of A600E C6 prior to regeneration and subjected to one of eight regeneration methods (R1a-R4a and R1b-R4b) using NaCl, summarized in SI Table S 4. The batch test variables included regeneration volume (4 or 20 BV), regeneration strength (1.4 or 2.0 N NaCl), and inclusion of a pre-regeneration batch test with 4 BV of a low strength NaCl solution (0.14 N or 0.2 N). R1-R2 used a single stage regeneration with a high concentration of NaCl (1.4 or 2 N) that varied the solution volume. R3-R4 used a two stage regeneration approach mimicking the flow-through regeneration with a low concentration solution (0.14 or 0.2 N) followed by a high concentration solution (1.4 or 2 N). After regeneration with one of the NaCl batch methods, sequential batch tests were also conducted using 6% wt. HCl. In these experiments, all solutions were prepared using type I or type II lab-grade water and reagent grade sodium chloride salt or 37% wt. HCl.

Table S 4: Batch test conditions for A600E C6 before regeneration resin

Regeneration Name	First Stage			Second Stage		
	Solution	Concentration (N)	BV	Solution	Concentration (N)	BV
R1a	NaCl (high)	1.4	20	-	-	-
R1b	NaCl (high)	2.0	20	-	-	-
R2a	NaCl (high)	1.4	4	-	-	-
R2b	NaCl (high)	2.0	4	-	-	-
R3a	NaCl (low)	0.14	4	NaCl (high)	1.4	20
R3b	NaCl (low)	0.2	4	NaCl (high)	2.0	20
R4a	NaCl (low)	0.14	4	NaCl (high)	1.4	4
R4b	NaCl (low)	0.2	4	NaCl (high)	2.0	4

1.5 Analytical methods

Sample analysis was performed by several laboratories over the course of the study (Table S 5) including Ana-Lab Corporation (Analab) (Kilgore, Texas), the Korak Lab at the University of Colorado Boulder (CU Boulder), the Interdisciplinary Center for Inductively Coupled Plasma-Mass Spectrometry at the University of California Davis, and the University of California Davis Analytical Lab (UC Davis). In general, samples were only analyzed at one location for each project task.

Sample analysis methods are summarized in Table S 6 for regeneration and batch tests. Metals samples were not digested but acidified to a concentration of 1% HNO_3 to measure total concentration. Regeneration and batch test samples analyzed at UC Davis and CU Boulder by EPA method 6020B used a modified method with multiple gas modes and a collision cell. Multiple gas modes include helium and hydrogen (which is specified in EPA6020B) and specifically allow for better analysis of chromium, selenium, arsenic, and vanadium. Multiple gas modes and collision cells both act to remove plasma-formed molecular ions with the same mass-to-charge ratio. Alkalinity measurements were adjusted for chromate-bichromate equilibrium.

Table S 5: Laboratories used for sample analysis

Column	Resin	Task				Reloading
		Loading	Regeneration	Batch Test		
				NaCl	HCl	
C1	**A600E**	Analab	N/A	UC Davis		N/A
C2	**A600E**	Analab	N/A	UC Davis		N/A
C3	**A600E**	Analab	UC Davis			CU Boulder
C4	**A600E**	Analab	N/A	UC Davis		N/A
C5	**A600E**	Analab	N/A			
C6	**A600E**	CU Boulder				N/A
C7	**PGW6002E**	Analab	UC Davis	UC Davis		CU Boulder
C8	**TP107**	Analab	UC Davis	UC Davis		CU Boulder

Table S 6: Methods used for sample analysis. SM = Standard Method.

Analyte	Lab and Method				
	Ana-Lab	**UC Davis**	**CU Boulder**	**Pilot Site**	**Regeneration Site**
pH	--	--	--	Meter at utility partner	Hach HQ40d
Total Alkalinity	--	--	--	Hach 8203	
Bicarbonate	--	SM 2320	--	--	--
Carbonate	--	SM 2320	--	--	--
Dissolved Oxygen	--	--	--	Meter at utility partner	--
TDS	--	--	--	SM 2540C	--
Conductivity	--	--	--	SM 2510B	SM 2510B; HachQ40d/IntelliCAL CDC401
DOC	SM 5310C	--	--	--	--
Calcium	EPA 200.7	modified EPA 6020B		--	--
Potassium	EPA 200.7	--	--	--	--
Magnesium	EPA 200.7	--	--	--	--
Sodium	EPA 200.7	modified EPA 6020B		--	--
Chloride	EPA 300.0		--	--	--
Sulfate	EPA 300.0		--	--	--
Nitrate	EPA 300.0		--	--	SM 4500B
Nitrate-Nitrite	EPA 300.0	--	--	--	--
Iron	EPA 200.7	--	--	--	--
Manganese	EPA 200.7	--		--	--
Arsenic	EPA 200.7	modified EPA 6020B		--	--
Chromium	EPA 200.7	modified EPA 6020B		--	--
Hexavalent chromium	EPA 218.6	--	--	--	--
Molybdenum	EPA 200.7	modified EPA 6020B		--	--
Selenium	EPA 200.7	modified EPA 6020B		--	--
Vanadium	EPA 200.7	modified EPA 6020B		--	--
Uranium	EPA 200.7	modified EPA 6020B		--	--
All analytes are unfiltered (total) concentrations unless noted. Modified EPA 6020B – analysis performed on ICP-MS with multiple gas modes and a collision cell					

2 Results

2.1 Column Loading with Fresh Resin

2.1.1 Chromium Loading – Biot Number

Dimensionless numbers can provide insight to the controlling kinetic mechanism. The Biot (Bi) number describes the contribution of internal diffusion resistance to external diffusion resistance and can be calculated using Equation S 1. The Bi number is a function of the fluid-phase mass transfer coefficient (k_f) (Equation S 2) which requires calculation of the Reynolds (Re) number (Equation S 3) and the Schmidt (Sc) number (Equation S 4). Raw water parameters were estimated using OLI: Stream Analyzer, and resin properties used publicly available data sheets from resin manufacturers (Table S 7).

$$\mathrm{Bi} = \frac{k_f r \tau}{\epsilon_p D_L^0} = \frac{\text{"Internal diffusion resistance"}}{\text{"External diffusion resistance"}} \qquad \text{Equation S 1}$$

$$k_f = \frac{[1+1.5(1-e)]D_L}{d}\left(2 + 0.644 * \mathrm{Re}^{1/2} * \mathrm{Sc}^{1/3}\right) \qquad \text{Equation S 2}$$

$$\mathrm{Re} = \frac{vd}{\nu e} \qquad \text{Equation S 3}$$

$$\mathrm{Sc} = \frac{\nu}{\rho D_L} \qquad \text{Equation S 4}$$

Calculating the Bi number required estimation of tortuosity (τ), bed void fraction (e), and water content (ϵ_p) using typical values for ion exchange resins (Sengupta, 2017) and the shipping water content provided by manufacturers (Table S 7). However, even when τ and ϵ_p are varied within a reasonable range (2-6 and 0.2 – 0.6, respectively), Bi numbers still generally exceed 30, except at very low tortuosity and high pore water content (Figure S 2).

Table S 7: Calculation of dimensionless numbers during loading

Parameter		Symbol	Units	Resin			Source
				A600E	PGW6002E	TP107	
Column parameters	**Velocity**	v	cm/s	1.02	0.54	0.54	Main Text Table 1
Raw water parameters	**Density**	ρ	kg/m^3	997.3	997.3	997.3	OLI
	Dynamic viscosity	η	kg/m/s	8.93×10^{-04}	8.93×10^{-04}	8.93×10^{-04}	OLI
	Kinematic viscosity	ν	m^2/s	8.96×10^{-07}	8.96×10^{-07}	8.96×10^{-07}	Calculation: $\frac{\eta}{\rho}$
	Diffusion Coefficient Chloride	D_L^o	m^2/s	2.01×10^{-09}	2.01×10^{-09}	2.01×10^{-09}	OLI
	Diffusion coefficient Chromium	D_L	m^2/s	1.09×10^{-09}	1.09×10^{-09}	1.09×10^{-09}	OLI
Resin properties	**Tortuosity**	τ	--	2-6	2-6	2-6	Estimate (Sengupta, 2017)
	Water content	ϵ_p	--	0.46 (0.2-0.6)	0.43 (0.2-0.6)	0.36 (0.2-0.6)	Shipping Water Content (Table S 1) and Estimate
	Diameter	d	mm	0.75	0.57	0.57	Manufacturer
	Bed void fraction	e	--	0.5	0.5	0.5	Estimate
Dimensionless numbers and calculated values	**Reynolds number**	Re	--	17.06	6.91	6.91	Equation S 3
	Schmidt number	Sc	--	820	820	820	Equation S 4
	External film mass transfer coefficient	k_f	m/s	6.86E-05	5.99E-05	5.99E-05	Equation S 2

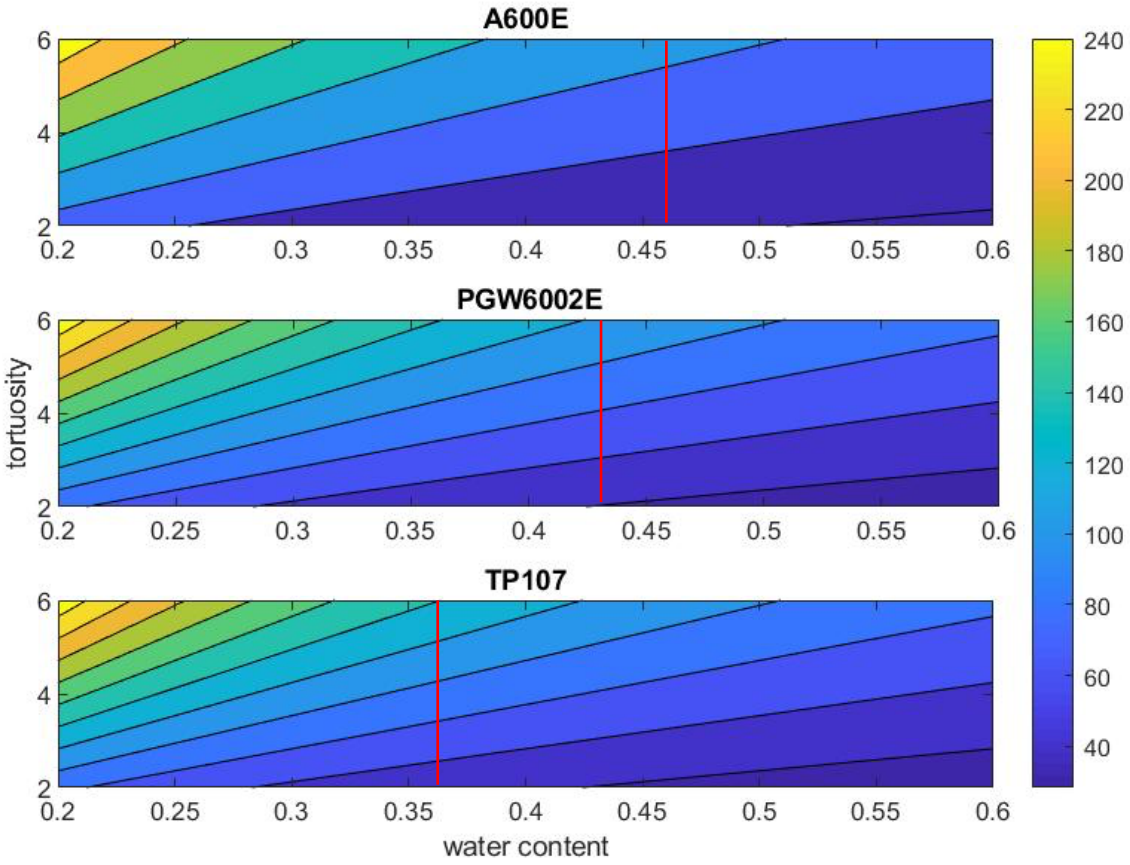

Figure S 2: Variation in Biot number as a function of tortuosity and pore water content. Vertical red lines denote average water content as reported by the manufacturer.

2.1.2 **Oxyanion Loading - A600E Resin**

In addition to chromium, breakthrough curves for arsenic, selenium, uranium, and vanadium were also evaluated for new A600E resin (C6) using high frequency sampling. Figure S 3 shows the breakthrough curve and cumulative amount loaded by integration. Samples below the minimum reporting limit were evaluated at half the MRL for cumulative loading calculations.

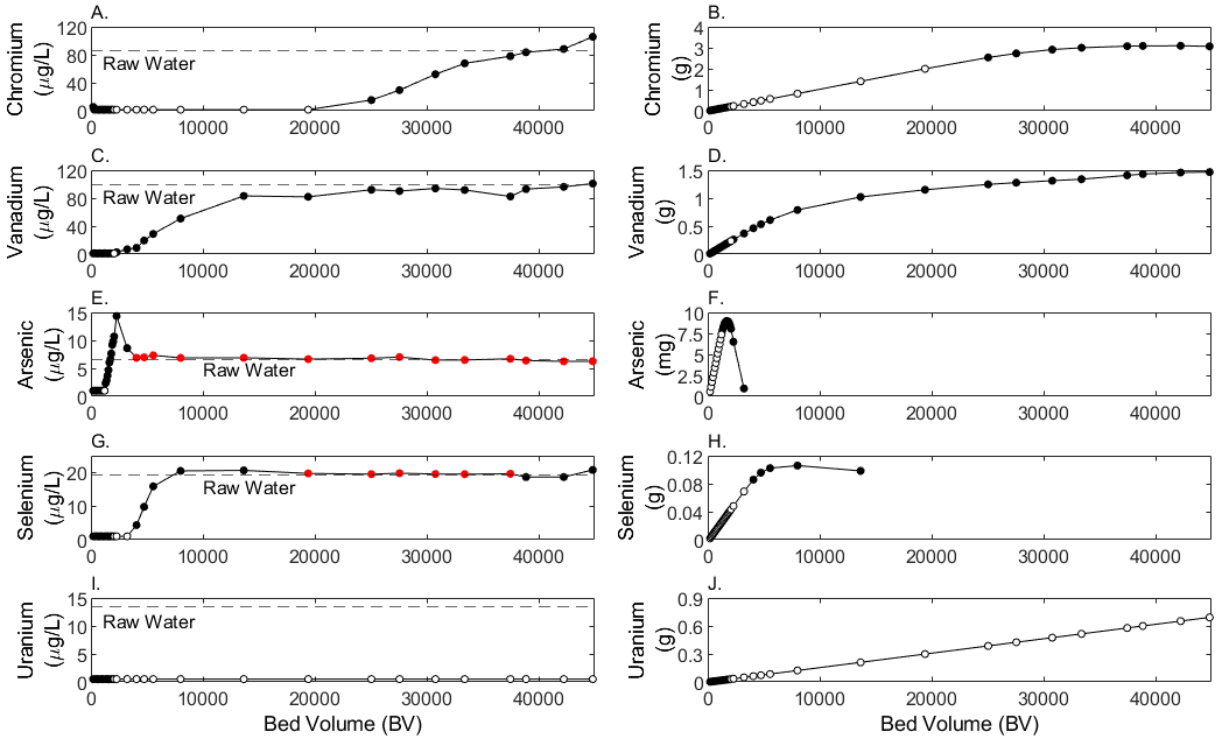

Figure S 3: A600E C6 loading breakthrough profiles (left column) and cumulative accumulation (right column) for chromium (A, B), vanadium (C, D), arsenic (E, F), selenium (G, H), and uranium (I, J). Red data points represent points within 5% of influent concentrations. Cumulative calculations ceased when effluent concentration asymptotically approached 5% of influent concentrations. Unfilled data points represent points below reporting limit. Dashed lines represent average influent concentration (Table S2).

Selenium. Selenium may have exhibited a small chromatographic peak during A600E loading (Figure S3). The maximum selenium concentration (20.6 µg/L) was 6% above the average influent concentration (19.4 µg/L) and more than 3 standard deviations from the raw water mean value. All selenium concentrations were far below the MCL for the U.S. (50 µg/L) but above maximum limits in the European Union (EU) (10 µg/L). Unlike arsenic, selenium release due to chromatographic peaking was minor. Selenium peaking depends on the oxidation state, where Se(IV) (e.g., SeO_3^{-2}) is less selective than sulfate and does chromatographically peak, and Se(VI) (e.g., SeO_4^{-2}) does not[69]. Therefore, a small chromatographic peak could be the result of multiple selenium forms in the raw water.

2.2 **Regeneration**

Bicarbonate and carbonate alkalinity were measured in regeneration effluent, adjusted for chromium speciation, and then cumulative elution of total carbonate was calculated for each regeneration phase (Table S 8).

Table S 8: Percent of total inorganic carbon recovered during each regeneration stage

Resin	0.2 N stage	2.0 N stage
A600E	89%	11%
PGW6002E	89%	11%
TP107	71%	29%
* Does not include extended regeneration for TP107		

Based on the integrated area under the regeneration curve, cumulative nitrate elution was highest for PGW6002E and lowest for TP107 (Figure 3I, main text). In contrast, TP107 eluted the most sulfate compared to PGW6002E and A600E (Figure 3H, main text). A common descriptor of anion exchange resins is the nitrate-sulfate separation factor[1,2], which describes monovalent-divalent selectivity. Assuming both nitrate and sulfate reach equilibrium during loading and that regeneration is completely efficient, the cumulative equivalents of nitrate and sulfate recovered are surrogates for resin-phase concentrations. Separation factor can then be calculated using raw water and resin-phase concentrations (Equation S5). TP107 has a higher divalent-monovalent separation factor (9.4) compared to A600E and PGW6002E (3.3 and 2.5, respectively). However, sulfate resin-phase concentrations were 1-2 orders of magnitude greater than nitrate, so only general comparisons should be made between resins.

$$\alpha_B^A = \frac{\bar{C}_A * C_B}{\bar{C}_B * C_A} \qquad \text{Equation S 5}$$

where,

α_B^A: separation factor of A relative to B
$\bar{C}_i$: resin phase concentration of constituent i
C_i: aqueous phase concentration of constituent i

2.3 Batch Test

2.3.1 Spatial Distribution

Sulfate. Spatial distribution of sulfate through columns prior to and following regeneration is shown in Figure S 4. Sulfate was not measured during HCl batch regenerations.

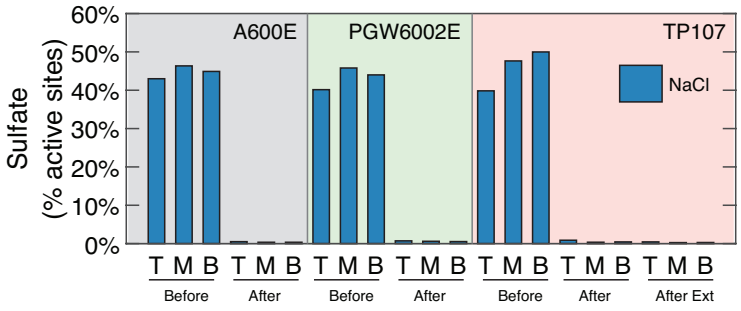

Figure S 4: Sulfate batch regeneration

Chromium Recovery with HCl. All batch tests recovered additional chromium with 6% wt HCl. This is inconsistent with prior work demonstrating lower selectivity reversal for chromium (as $HCrO_4^-$) in acidic solutions with high ionic strength[3], illustrating a limitation of relying on a single batch test as an indicator of either resin-phase concentrations or regeneration efficiency. During NaCl regeneration of pre-regeneration resin aliquots, liquid-phase concentrations were high (86-105 mg/L) leaving a non-trivial amount of chromium on the resin to be recovered with HCl. In this case, higher recovery during HCl batch tests may falsely appear like a fraction of chromium is thermodynamically unfavorable to be recovered during NaCl column regeneration. When liquid-phase concentrations are high, a second sequential batch regeneration with NaCl would give a more representative value of resin-phase concentration.

2.3.2 Batch Regeneration Approach

Batch tests provide a direct measurement of resin-phase concentrations, assuming that recovery in the liquid phase is near 100% complete. Comparing the different batch test methods (Table S 4 and Figure S 5), overall recovery of chromium and vanadium was not impacted by a 42% change in regenerant strength (2.0 N vs. 1.4 N), but recovery was impacted by regenerant volume. With 4 BV of 2.0 N or 1.4 N NaCl (R2a and b), recovery decreased 23-31% for chromium and 35-53% for vanadium compared to 20 BV of the same strength NaCl (R1a and b). Using an excess of regenerant (e.g., 5 times more volume than column regeneration) decreases liquid-phase concentrations at equilibrium and improves recovery.

Vanadium recovery with HCl increased by up to 3.6x when a 0.2 N NaCl batch regeneration preceded the 2 N NaCl batch regeneration, suggesting the form or selectivity of vanadium may be impacted by the low strength (i.e., 0.2 N) regeneration stage. Therefore, increased focus on batch tests could improve understanding of resin-phase behaviors for complex constituents like vanadium. Regeneration efficiency calculations (main text Section 4.1) only use results from R1a (20 BV of 2.0 N NaCl), as this approach has the simplest procedure by skipping the 0.2 N NaCl step and reduces experimental bias by using the larger NaCl regenerant volume.

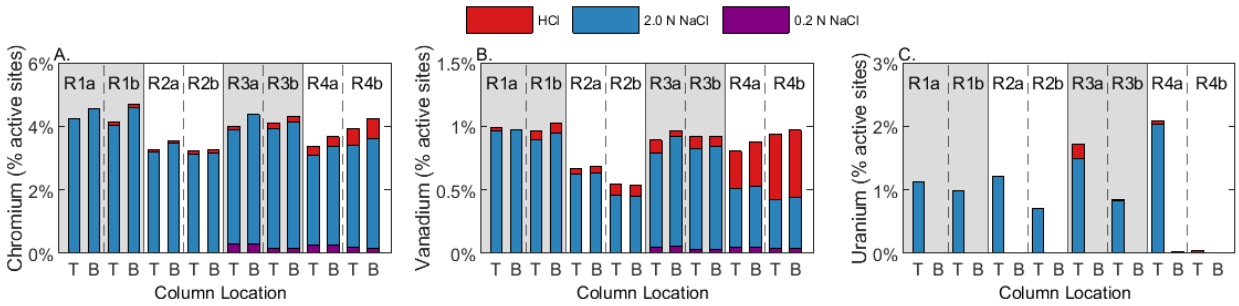

Figure S 5: Resin phase concentrations by regeneration approach using A600E C6 pre-regeneration resin aliquots for (A) chromium, (B) vanadium, and (C) uranium. T and B denote top and bottom. Shaded regions represent the specific regeneration approach (e.g., R1a), corresponding to Table S 4.

3 Practical Implications

3.1 Regeneration Efficiency

Calculating regeneration efficiency requires an estimate of cumulative mass loaded and mass recovered during regeneration. Using the parameters measured in this study, cumulative loading can be estimated by two approaches. Approach L1 integrates the breakthrough curve during loading using Equation 2 (main text). Approach L2 estimates the mass loaded by integrating the regeneration elution profile and adding the additional mass recovered from post-regeneration batch tests on resin aliquots using Equations 3 and 4 in the main text. Table S 9 summarizes cumulative loading of uranium, vanadium, and chromium to each resin.

Table S 9: Estimates of cumulative loading (m_{load}) for regeneration efficiency calculations

Resin	Uranium [g U/L_{resin}]	Vanadium [g V/L_{resin}]	Chromium [g Cr/L_{resin}]	
	L1	L2	L1	L2
A600E	0.53	1.44	2.36	2.66
PGW6002E	0.82	1.93	3.65	2.73
TP107	1.85	5.04	8.08	7.25
TP107 (extended)	1.85	4.77	8.08	7.25

3.2 Staggered Contactors

Breakthrough curves for both chromium and arsenic were used to simulate the operation of multiple contactors with staggered regeneration. Chromium curves from the initial loading and arsenic curves during reloading were used for modeling. Arsenic was only measured during reloading for PGW6002E and TP107, and reloading had better data resolution (and a similar profile compared to the initial loading) for A600E (Section 3.3.2). By offsetting multiple contactors in parallel, the chromatographic peak for arsenic can be dampened by the flow from other contactors. The total throughput for each contactor can also increase, because the breakthrough of chromium from one reactor is diluted by the effluent from other contactors that have not yet started to breakthrough.

To model a staggered configuration, the pilot-scale data was first standardized. The chromium breakthrough profiles for new resin were smoothed using the locally estimated scatter smoothing (LOESS) method with 30% of the data for each subset. The smoothed data was then interpolated over a regular interval of bed volumes (50 BV). Before breakthrough, the data was

censored to a project reporting limit of 3 µg/L. Using the MRL is a conservative approach, because it will overestimate concentrations at early bed volumes. After breakthrough, the concentration was assumed constant at the average raw water concentration (87 µg/L). Figure S 6 compares the experimental data against the standardized data for modeling.

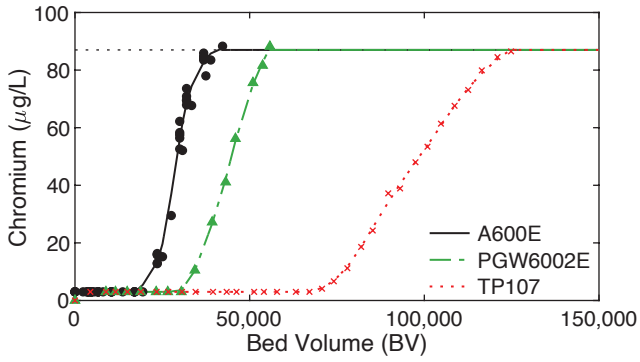

Figure S 6. Comparison for experimental measurements (markers) and smoothed data (line) for chromium across all three resins. Dashed line is the average raw water concentration.

A similar approach was used to standardize the arsenic data for modeling (Figure S 7). The high frequency data collected during reloading was used for all three resins, because arsenic chromatographic peaking was not measured on fresh resin for PGW6002E or TP107. Similar to the chromium data set, concentrations below the reporting limit were censored at 2 µg/L. After complete breakthrough, the concentration was set to the average raw water concentration (6.6 µg/L) for the remainder of the run as chromium broke through. There were varying degrees of sampling resolution during chromatographic peaking. A second order polynomial was fit to the data above the raw water concentration to estimate the magnitude and duration of the peak. For A600E, which had the best sampling resolution across the peak, this approach agreed well with the measured concentrations (Figure S 7). Comparatively, PGW6002E and TP107 peaked later and have fewer measured concentrations at higher bed volumes. For PGW6002E, fitting a polynomial for concentrations up to 3,100 BV also agreed with the measured concentration at 3,700 BV. TP107 has the most uncertainty due to the fewest observation past 4,000 BV.

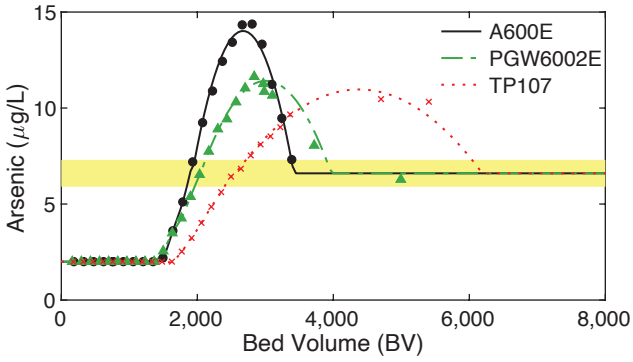

Figure S 7. Comparison for experimental measurements (markers) and smoothed data (line) for chromium across all three resins. The shaded region is the average raw water concentration plus/minus one standard deviation.

Using these smoothed breakthrough curves, the blended concentrations from the staggered contactors were modeled in MATLAB. The modeling approach used an iterative solver. Given the number of contactors and offset between contactors, the total number of bed volumes that could be processed through each single contactor was solved iteratively, such that the maximum

blended effluent concentration for chromium was the treatment objective (8 or 10 µg/L). Using this total throughput for each contactor, the maximum blended arsenic concentration was calculated. Equal flow through each contactor is assumed.

For example, Figure S 8 shows the simulation results for A600E with 2 contactors in parallel offset by 3,500 BV. Contactor 1 starts loading at 0 BV and starts to breakthrough about 16,000 BV. Contactor 2 is delayed by 3500 BV. Contactor 2 is regenerated 3,500 BV into the loading cycle for Contactor 1 as indicated by the vertical line. The non-linear solver in Matlab iteratively adjusts the total throughput for each contactor (i.e., 23,560 BV for this scenario) until the maximum combined effluent is 10 µg/L for chromium. In this scenario, however, the maximum arsenic concentration is 10.3 µg/L and would exceed the MCL. Therefore, this treatment configuration is not viable.

When 3 contactors are offset by 3,500 BV (Figure S 9), this combination achieves treatment objectives for both chromium and arsenic concentrations less than 10 µg/L. With this scenario, each contactor can load for 24,660 BV maintaining a blended chromium concentration less than 10 µg/L. In this scenario, staggering 3 contactors yields a maximum arsenic concentration of 9.1 µg/L and meets the MCL for arsenic.

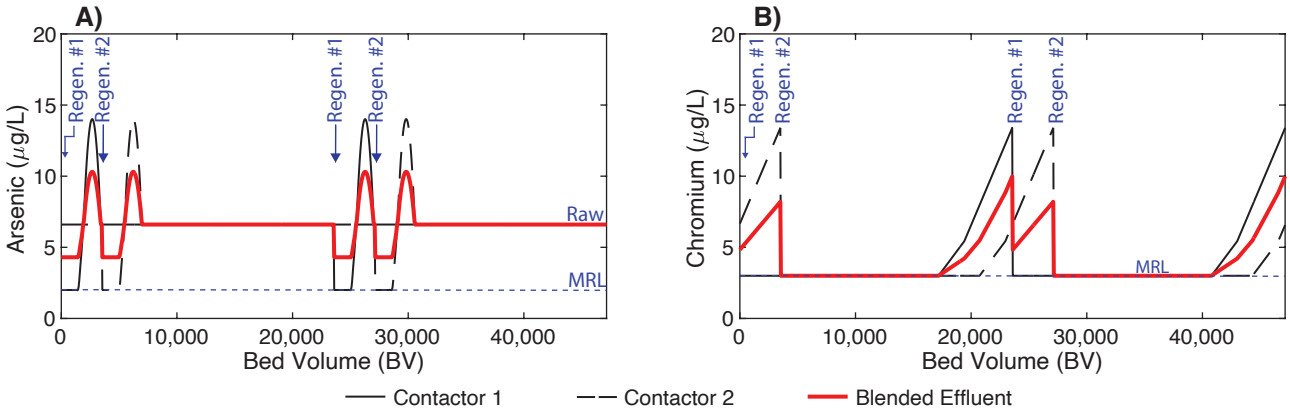

Figure S 8. Staggered contactor simulation results for A600E with 2 contactors offset by 3,500 BV.

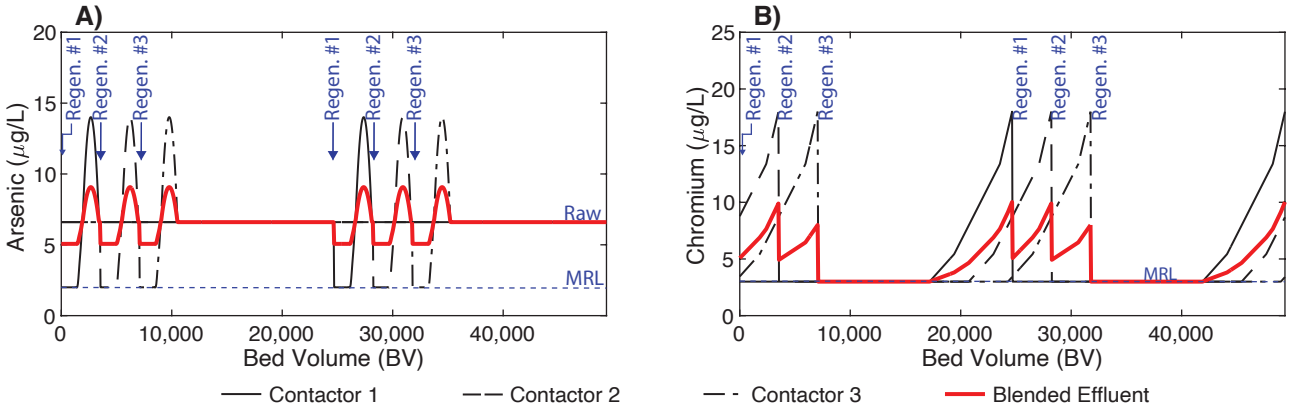

Figure S 9. Staggered contactor simulation results for A600E with 3 contactors offset by 3,500 BV.

Figure 7 in the main text performs this analysis for all three resins across a wide range of configurations. The number of contactors ranges from 2 to 10, and the contactor offset ranges from 500 to 45,000 BV. The graphical heat maps show which configurations cannot meet the

arsenic MCL (black), are infeasible for chromium (white), and viable (color scale). The color scale shows how many bed volumes each contactor can treat and meet 10 µg/L objectives for chromium and arsenic, revealing trends between configuration and overall resin utilization. Figure S 10 shows the sensitivity to the treatment objective by implementing a safety factor that decreases the treatment objectives to 8 µg/L. With the safety factor, all resins need at least 4-5 contactors to meet the arsenic MCL. The maximum throughput for each contactor also decreases to meet the chromium target.

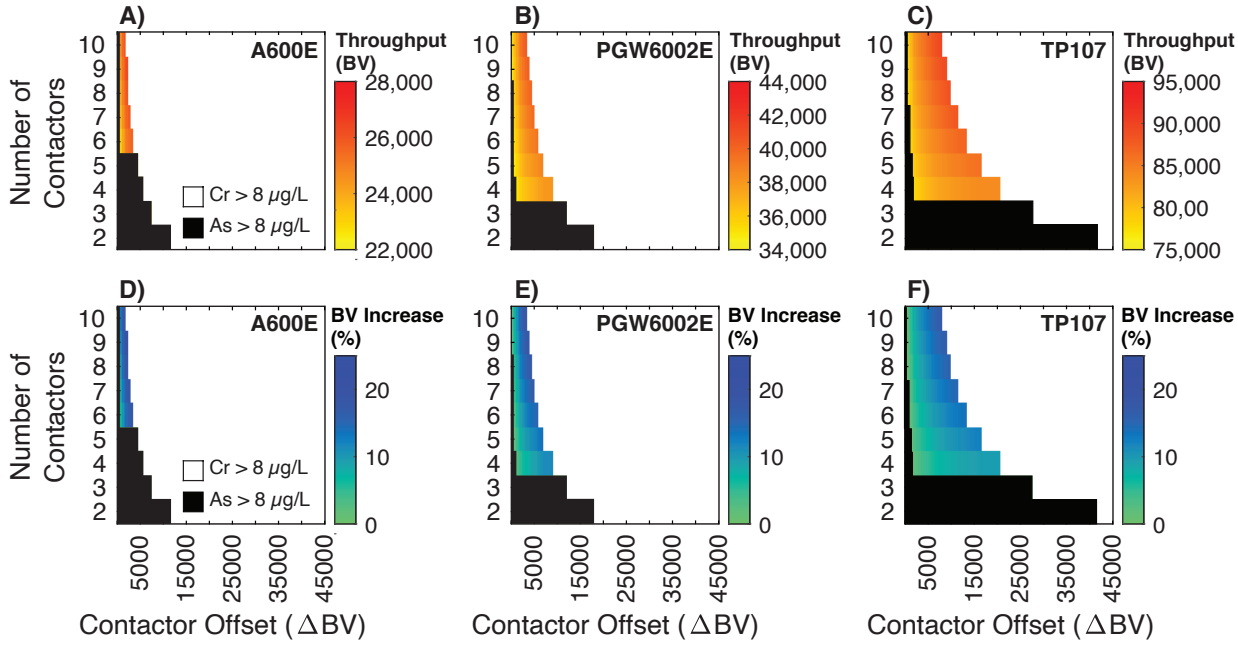

Figure S 10. Heat maps of model results for the staggered contactor analysis for a 20% safety factor decreasing the treatment objective to 8 µg/L for both arsenic and chromium. Color bar represents the maximum throughput for each contactor or the relative increase in resin utilization (i.e., throughput) compared to one column operating to 8 µg/L chromium. for different combinations of number of contactors and offset between the contactors.

3.3 Uranium Accumulation

Radioactive waste disposal regulations vary by location, but in the U.S., a material containing above 0.05% by weight uranium may require controlled disposal[4]. Uranium accumulation is typically considered in the context of single-use weak base resins with 100,000-200,000 BV of loading[5,6], but this study shows the importance in regenerable resins with low regeneration efficiency for uranium, even when uranium concentrations are below regulatory limits in the raw water. Accumulation over successive loading cycles was estimated using Equation S6 with three assumptions: 1) uranium is completely removed from the raw water during loading (Section 3.1.2), 2) loading throughput for each cycle is constant, and 3) regeneration efficiency each cycle is a constant percentage (Table 4). Uranium concentrations are averaged across bed depth.

$$W_U(n) = \left(M_U(n) * e_{regen_U} * \rho\right) * 100\% + W_U(n-1) \qquad \text{Equation 7}$$

where,

n and $(n-1)$: The current and prior loading and regeneration cycles, respectively

$W_U(n)$: Weight percent of uranium following the nth loading and regeneration cycle

M_U: Mass of uranium loaded

ρ: Resin density as reported by the manufacturer

e_{regen_U}: Uranium regeneration efficiency

Two scenarios were considered: a worst-case scenario with loading to full chromium breakthrough (e.g., in a lead-lag scenario) and a best-case scenario with chromium loading to 10 µg/L. Under both, PGW6002E and TP107 both exceed 0.05% wt uranium after the first loading-regeneration cycle (Figure S11). A600E reaches this limit after 2 or 3 cycles for each scenario, respectively. Assuming regeneration efficiency is constant, uranium accumulation could level off after few cycles for resins with higher regeneration efficiencies. Acid or carbonate supplemented regeneration can recover additional uranium after NaCl regeneration[7], and a utility may periodically need to perform an atypical regeneration to manage uranium accumulation.

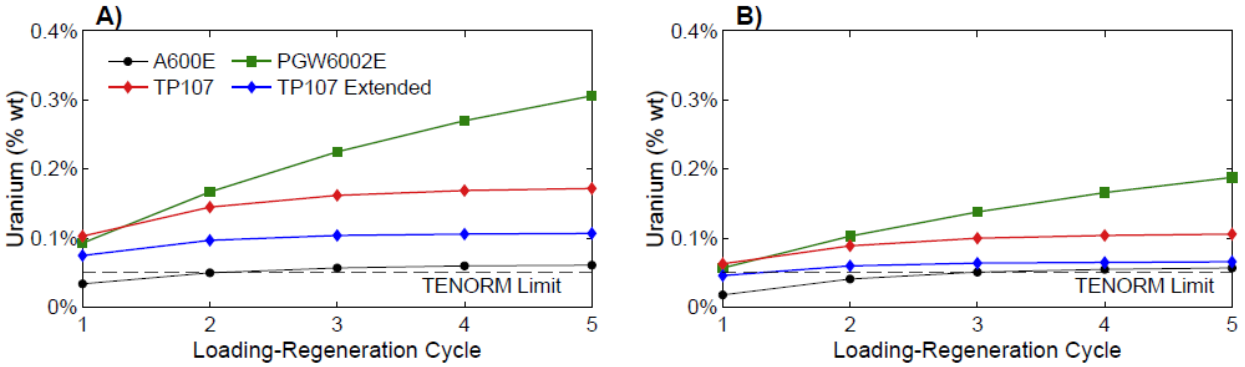

Figure S11: Uranium accumulation through successive loading and regeneration cycles for (A) a worst-case scenario where columns are loaded to full chromium exhaustion, and (B) a best-case scenario where columns are loaded to 10 µg/L chromium breakthrough

4 References

(1) Clifford, D.; Weber, W. J. The Determinants of Divalent/Monovalent Selectivity in Anion Exchangers. *Reactive Polymers, Ion Exchangers, Sorbents* 1983, *1* (2), 77–89. https://doi.org/10.1016/0167-6989(83)90040-5.

(2) Subramonian, S.; Clifford, D. Monovalent/Divalent Selectivity and the Charge Separation Concept. *Reactive Polymers, Ion Exchangers, Sorbents* 1988, *9* (2), 195–209. https://doi.org/10.1016/0167-6989(88)90033-5.

(3) SenGupta, A. K.; Clifford, D. A. Important Process Variables in Chromate Ion Exchange. *Environmental Science & Technology* 1986, *20* (2), 155–160. https://doi.org/https://doi.org/10.1021/es00144a006.

(4) USEPA. *A Regulators' Guide to the Management of Radioactive Residuals from Drinking Water Treatment Technologies*; EPA Report EPA 816-R-05-004, 2005.

(5) Najm, I.; Brown, N. P.; Seo, E.; Gallagher, B.; Gramith, K.; Blute, N. K.; Wu, X.; Yoo, M.; Liang, S.; Maceiko, S.; Kader, S.; Lowry, J. Impact of Water Quality on Hexavalent Chromium Removal Efficiency and Cost. *Water Research Foundation Project #4450* 2014, 1–174.

(6) Blute, N. K.; Wu, X.; Imamura, G.; Song, Y.; Porter, K.; Fong, L.; Froelich, D.; Abueg, R.; Henrie, T.; Ramesh, S.; Vallejo, F. Assessment of Ion Exchange, Adsorptive Media, and RCF for Cr(VI) Removal. *Water Research Foundation Project #4423* 2015, 1–158.

(7) Korak, J. A.; Huggins, R.; Arias-Paic, M. Regeneration of Pilot-Scale Ion Exchange Columns for Hexavalent Chromium Removal. *Water Research* 2017, *118*, 141–151. https://doi.org/10.1016/j.watres.2017.03.018.